

Rational design of layered oxide materials for sodium-ion batteries

Zhao, Chenglong; Wang, Qidi; Yao, Zhenpeng; Wang, Jianlin; Sánchez-Lengeling, Benjamín; Ding, Feixiang; Qi, Xingguo; Lu, Yaxiang; Wagemaker, Marnix; More Authors

DOI

[10.1126/science.aay9972](https://doi.org/10.1126/science.aay9972)

Publication date

2020

Document Version

Accepted author manuscript

Published in

Science

Citation (APA)

Zhao, C., Wang, Q., Yao, Z., Wang, J., Sánchez-Lengeling, B., Ding, F., Qi, X., Lu, Y., Wagemaker, M., & More Authors (2020). Rational design of layered oxide materials for sodium-ion batteries. *Science*, 370(6517), 708-711. <https://doi.org/10.1126/science.aay9972>

Important note

To cite this publication, please use the final published version (if applicable).
Please check the document version above.

Copyright

Other than for strictly personal use, it is not permitted to download, forward or distribute the text or part of it, without the consent of the author(s) and/or copyright holder(s), unless the work is under an open content license such as Creative Commons.

Takedown policy

Please contact us and provide details if you believe this document breaches copyrights.
We will remove access to the work immediately and investigate your claim.

Rational design of layered oxide materials for sodium-ion batteries

Chenglong Zhao^{1,2,†}, Qidi Wang^{3,4,†}, Zhenpeng Yao^{5,†}, Jianlin Wang⁶, Benjamín Sánchez-Lengeling⁵, Feixiang Ding^{1,2}, Xingguo Qi^{1,2}, Yaxiang Lu^{1,2*}, Xuedong Bai⁶, Baohua Li³, Hong Li^{1,2}, Alán Aspuru-Guzik^{5,7*}, Xuejie Huang^{1,2}, Claude Delmas^{8*}, Marnix Wagemaker^{9*}, Liquan Chen¹, and Yong-Sheng Hu^{1,2,10*}

Affiliations:

¹Key Laboratory for Renewable Energy, Beijing Key Laboratory for New Energy Materials and Devices, Beijing National Laboratory for Condensed Matter Physics, Institute of Physics, Chinese Academy of Sciences, Beijing 100190, China.

²Center of Materials Science and Optoelectronics Engineering, University of Chinese Academy of Sciences, Beijing 100049, China.

³Shenzhen Key Laboratory on Power Battery Safety and Shenzhen Geim Graphene Center, School of Shenzhen International Graduate, Tsinghua University, Guangdong 518055, China.

⁴School of Materials Science and Engineering, Tsinghua University, Beijing 100084, China.

⁵Department of Chemistry and Chemical Biology, Harvard University, Cambridge, MA, 02138, USA.

⁶State Key Laboratory for Surface Physics, Institute of Physics, Chinese Academy of Sciences, Beijing, 100190, China.

⁷Department of Chemistry and Department of Computer Science, University of Toronto, Toronto, Ontario M5S 3H6, Canada.

⁸Université de Bordeaux, Bordeaux INP, ICMCB UMR 5026, CNRS, 33600 Pessac, France.

⁹Department of Radiation Science and Technology, Delft University of Technology, Mekelweg 15, 2629JB Delft, the Netherlands.

¹⁰Yangtze River Delta Physics Research Center Co. Ltd, Liyang 213300, China.

Corresponding authors: yxlu@iphy.ac.cn, aspuru@utoronto.ca, delmas@icmcb-bordeaux.cnrs.fr, m.wagemaker@tudelft.nl, yshu@iphy.ac.cn

[†]C.Z., Q.W., and Z.Y. contributed equally to this work.

Abstract: Sodium-ion batteries have captured widespread attention for grid-scale energy storage owing to the natural abundance of sodium. The performance of such batteries is limited by available electrode materials, especially for sodium-ion layered oxides, motivating the exploration of high compositional diversity. How the composition determines the structural chemistry is decisive for the electrochemical performance, but very challenging to predict especially for complex compositions. We introduce the “cationic potential” that captures the key interactions of layered materials, and makes it possible to predict the stacking structures. This is demonstrated through the rational design and preparation of layered electrode materials with improved performance. As the stacking structure determines the functional properties, this methodology offers a solution towards the design of alkali metal layered oxides.

One Sentence Summary:

A general strategy is proposed for the design of sodium-ion layered oxide materials.

Integration of intermittent renewable energy sources demands the development of sustainable electrical energy storage systems(1). Compared to lithium (Li)-ion batteries, the abundance and low cost of sodium (Na) make Na-ion batteries promising for smart grids and grid-scale applications(2, 3). Li-ion layered oxides, with the general formula LiTMO_2 , have represented the dominant family of electrode materials for Li-ion batteries since 1980(4). Here TM stands for one or multiple transition metal elements that facilitate the redox reaction associated with Li-ion (de-)intercalation. The layered structures are built up by edge-sharing TMO_6 octahedra, forming repeating layers between which Li ions are positioned in the octahedral (O) oxygen environment, leading to the so-called O-type stacking. The structure offers high compositional diversity, providing tuneable electrochemical performance, where well-known examples are LiCoO_2 and Ni-rich $\text{LiNi}_y\text{Co}_z\text{Mn}(\text{Al})_{1-y-z}\text{O}_2$. In search of electrodes for Na-ion batteries, layered oxides (Na_xTMO_2) offered the natural starting point(5). However, a key difference is that for Na-ion oxides in addition to O-type, P-type stacking can occur, where P-type refers to prismatic Na-ion coordination (Fig. 1A). These stackings show distinctly different electrode performance, where the most studied layered stacking configurations are P2 and O3 types (Fig. 1A), referring to the ABBA and ABCABC oxygen stacking, respectively(6). P2-type oxides usually provide higher Na-ion conductivity and better structural integrity against the O3 analogues, which is responsible for the high power density and good cycling stability(7). However, the lower initial Na content of P2-type electrodes limits the reversible capacity in the first charge compared to high Na-content O3-type materials(8). Usually, the structural transition between the O- and P-type can occur upon Na-ion (de)intercalation during (dis)charging, typically degrading cycle stability(2, 3).

In search for electrodes with good chemical/dynamic stability and high Na storage performance, various P2- and O3-type Na-ion layered oxides have been synthesized and investigated(9, 10). However, effective guidelines towards the design and preparation of optimal electrode materials are lacking. Crystal structures of P2- and O3-type layered oxides can be differentiated based on the ratio between the interlayer distance of the Na metal layer $d_{(\text{O}-\text{Na}-\text{O})}$ and the TM layer distance $d_{(\text{O}-\text{TM}-\text{O})}$ (11), where a ratio of ~ 1.62 distinguishes P2- and O3-type oxides (Fig. S1 and Table S1)(12). The larger ratio of P2-type oxides, originates from the more localized electron distribution within the TMO_2 slabs, which results in a weaker repulsion between the adjacent NaO_2 slabs and consequentially a stronger repulsion between the adjacent TMO_2 slabs. This hints that the electron

distribution plays an important role in the competition between the P- and O-type stackings in layered oxides.

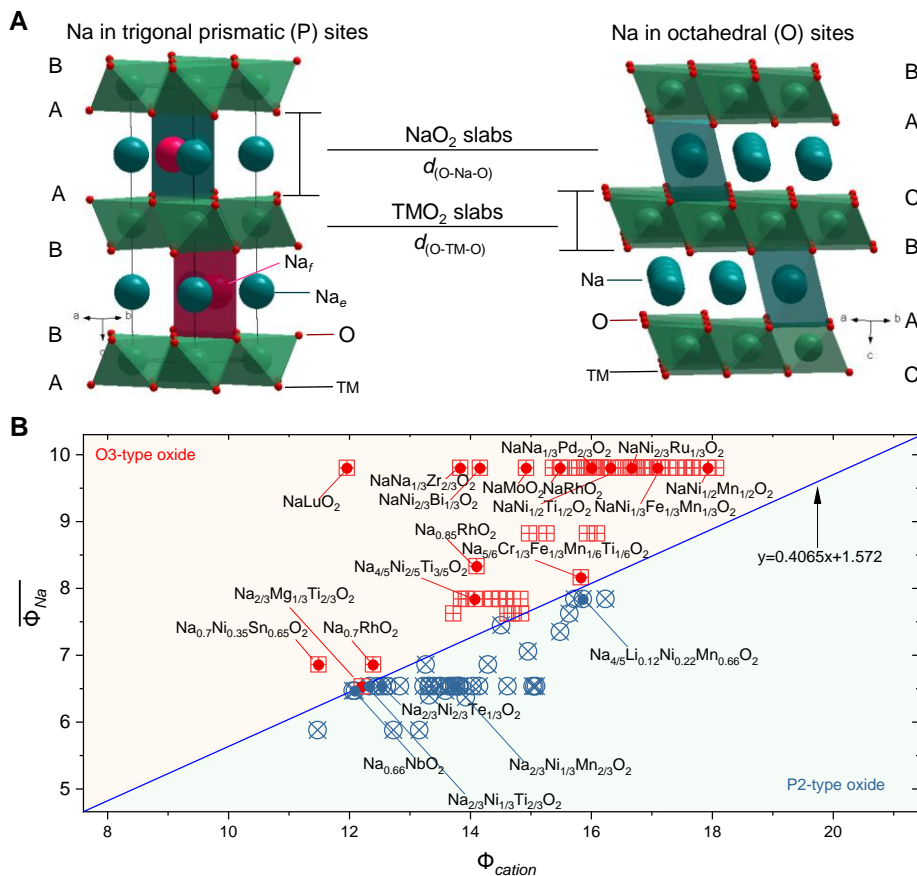


Fig. 1. Ionic potential and its use in Na-ion layered oxides. (A) Schematic illustration of crystal representative P2-type (hexagonal) and O3-type (rhombohedral) layered oxides. (B) Cationic potential of representative P2- and O3-type Na-ion layered oxides, considering the Na content, oxidation state of transition metals and TMs composition (see Supplementary text and Fig. S3 for details).

Ionic potential (Φ) is an indicator of the charge density at the surface of an ion, which is the ratio of the charge number (n) with the ion radius (R) introduced by G. H. Cartledge⁽¹³⁾, reflecting the cation polarization power. The ionic potential shows the expected increase with oxidation state and atom mass (Fig. S2 and Table S2), a consequence of the less localized orbitals.

Aiming at a simple descriptor for layered oxides, we express the extent of the cation electron density and its polarizability, normalized to the ionic potential anion(O), by defining the ‘‘cationic potential’’:

$$\Phi_{\text{cation}} = \frac{\overline{\Phi_{\text{TM}} \Phi_{\text{Na}}}}{\Phi_{\text{O}}} \quad (1)$$

where $\overline{\Phi_{TM}}$ represents the weighted average ionic potential of TMs, defined as $\overline{\Phi_{TM}} = \sum \frac{w_i n_i}{R_i}$, w_i is the content of TM_i having charge number n_i and radius R_i , and $\overline{\Phi_{Na}}$ represents the weighted average ionic potential of Na defined as $\overline{\Phi_{Na}} = \frac{x}{R_{Na}}$. Charge balance in Na_xTMO_2 composition demands $\sum w_i n_i = 4 - x$, where x represents Na content and 4 is the total oxidation state to charge compensate O^{2-} .

The cationic potential Φ_{cation} vs. the average Na ionic potential $\overline{\Phi_{Na}}$ of reported P2- and O3-type layered oxides results in the phase map shown in Fig. 1B. The distinct P2 and O3-type regions indicate that the cationic potential is an accurate descriptor of the inter-slab interaction, and thereby the structural competition between P2- and O3-type structures. A larger cationic potential (Eq.1), implies stronger TM electron cloud extend and interlayer electrostatic repulsion resulting in the P2-type structure, with more covalent TM-O bonds and an increased $d_{(O-Na-O)}$ distance (Fig. S4). Opposing this, a larger mean Na ionic potential, achieved by increasing Na content, increases the shielding of the electrostatic repulsion between the TMO_2 slabs, favouring the O3-type structure.

The phase map (Fig. 1B) shows that very small differences in TM or Na content can result in a transition between P2- and O3-type structures. To illustrate this we consider layered oxides with the composition $Na_{2/3}TMO_2$, which typically crystallizes in P2-type structure for the low Na content, such as P2- $Na_{2/3}CoO_2$ (14), P2- $Na_{2/3}Ni_{1/3}Ti_{2/3}O_2$ (15), etc. However, replacing Ni^{2+} with Mg^{2+} in P2- $Na_{2/3}Ni_{1/3}Ti_{2/3}O_2$, facilitated by their similar ionic radii(16), leads to $Na_{2/3}Mg_{1/3}Ti_{2/3}O_2$ for which the cationic potential predicts the O3-type structure, which is difficult to predict even with complex electrostatic energy calculations(15). In this case, the smaller ionic potential of Mg^{2+} against Ni^{2+} (Fig. 1B) decreases Φ_{cation} ; the resulting lower covalence of Mg/Ti-O bonds increases the charge carried by the oxygens and thereby weakens the repulsion between the TM layers, resulting in O3-type structure (Fig. S5A and B, Table S6 and S7). Substituting 1/6 Mg^{2+} by Ni^{2+} in $Na_{2/3}Mg_{1/3}Ti_{2/3}O_2$ to $Na_{2/3}Ni_{1/6}Mg_{1/6}Ti_{2/3}O_2$ moves it back into P2-type structure (Fig. S5B), illustrating how near these compositions are to the line separating the P2 and O3-type phases. Several other examples demonstrating that the proposed cationic potential approach captures the subtle balance between the P2- and O3-type layered Na_xTMO_2 structures are provided in the Supplementary text, Fig. S5C and Fig. S6.

Delmas et al.(6, 17) used the Rouxel diagram(18) to distinguish Na_xTMO_2 stacking structures, demonstrating that both Na content and the ionicity/covalence of bonds are the important factors. However, this method only accounts for the difference in Pauling's electronegativity (Fig. S7 and Table S4), that makes it impossible to predict the structure of oxides with the same TMs in different oxidation states(6, 17) (e.g., Mn^{4+} and Mn^{3+} in $Na_{0.7}MnO_2$) or for multiple-component systems (see Supplementary text, Fig. S8 and Table S5 for details). The cationic potential correctly predicts the stacking structure for these cases, providing a guideline for the development of Na-ion layered oxides.

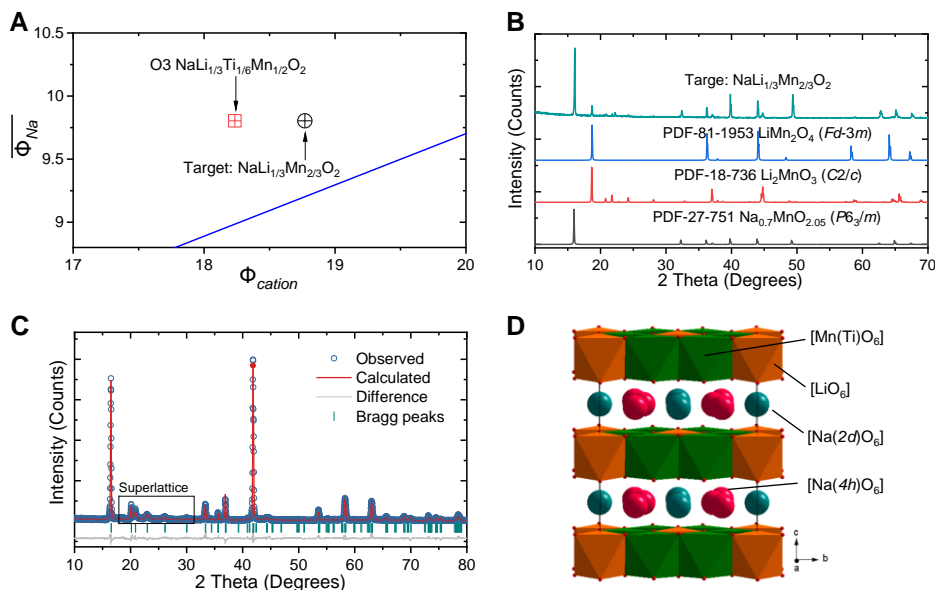


Fig. 2. Designing an O3-type oxide. (A) Analysis of the cationic potential of Na-Li-Mn(Ti)-O oxides (see Table S8 and S9 for details). (B) X-ray diffraction (XRD) patterns of the targeted $\text{NaLi}_{1/3}\text{Mn}_{2/3}\text{O}_2$ and the standard references. (C) Rietveld refinement of XRD pattern of $\text{NaLi}_{1/3}\text{Ti}_{1/6}\text{Mn}_{1/2}\text{O}_2$ (see Table S10-12 for details). (D) Schematic illustration of the corresponding structure with the Li/Mn(Ti) ordering in the $[\text{Li}_{1/3}\text{Ti}_{1/6}\text{Mn}_{1/2}]\text{O}_2$ slabs.

Using the cationic potential as guide, we design specific stacking structures by controlling the Na content and TM composition. An interesting starting point is $\text{NaLi}_{1/3}\text{Mn}_{2/3}\text{O}_2$, the analogue of $\text{LiLi}_{1/3}\text{Mn}_{2/3}\text{O}_2$ (Li_2MnO_3), providing capacity based on oxygen redox chemistry. This composition has not been prepared so far, despite that theoretical calculations argue $\text{NaLi}_{1/3}\text{Mn}_{2/3}\text{O}_2$ is stable in O3-type structure⁽¹⁹⁾. Various experimental conditions were attempted to prepare this composition in O3-type structure, but always a P2-type component, in addition to other phases was obtained. Lowering the cationic potential suggests that a possible route to prepare the O3-type structure is partial substitution of Mn^{4+} by Ti^{4+} (Fig. 2A), where Ti^{4+} has a lower ionic potential. $\text{NaLi}_{1/3}\text{Ti}_{1/6}\text{Mn}_{1/2}\text{O}_2$ was successfully prepared in the predicted O3-type structure (Fig. 1B) by a typical solid-state reaction (see the Methods). Notably, $\text{NaLi}_{1/3}\text{Mn}_{2/3}\text{O}_2$ could not be synthesized as an O3-type structure using the same method (Fig. 2B). Rietveld refinement of the XRD pattern confirmed the layered rock-salt structure (Fig. 2C), in which the NaO_2 layers alternate with the mixed $[\text{Li}_{1/3}\text{Ti}_{1/6}\text{Mn}_{1/2}]\text{O}_2$ slabs (Fig. 2D). The $(1/3, 1/3, l)$ superstructure peaks in $20\text{-}30^\circ$ suggest Li/Mn(Ti) ordering in a honeycomb pattern, which is also confirmed by the aberration-corrected scanning transmission electron microscopy (Fig. S9). This ordered arrangement of Li and Mn(Ti) in the TMO_2 slabs has not been observed in O3-type Na-ion oxides with exclusively $3d$ TMs. The electrochemical properties (see Supplementary text and Fig. S10A for details), demonstrate a higher energy density of $\sim 630 \text{ Wh kg}^{-1}$ than the reported O3-type electrodes.

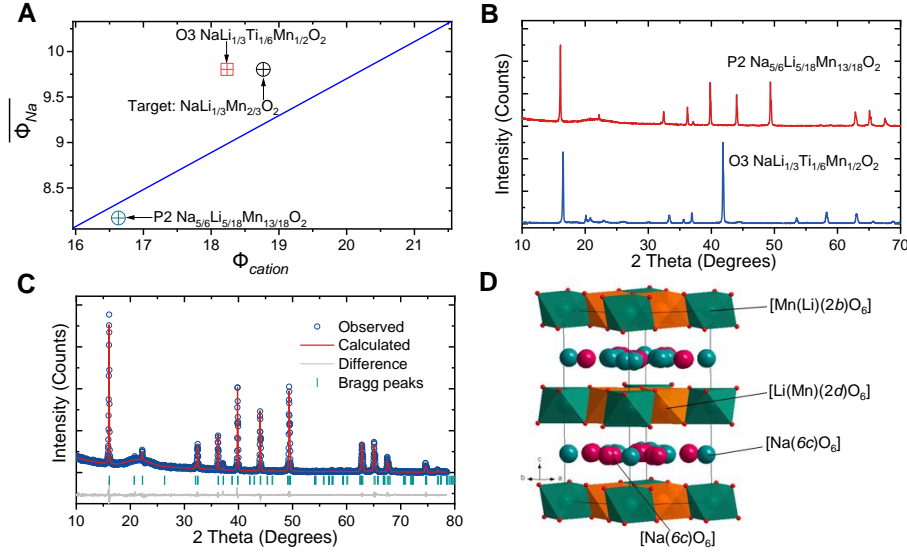


Fig. 3. Designing P2-type oxide. (A) Analysis of cationic potential of Na-Li-Mn-O oxides (see Table S13 and S14 for details). (B) XRD patterns of $\text{NaLi}_{1/3}\text{Ti}_{1/6}\text{Mn}_{1/2}\text{O}_2$ and $\text{Na}_{5/6}\text{Li}_{5/18}\text{Mn}_{13/18}\text{O}_2$ oxides. (C) Rietveld refinement of XRD pattern of $\text{Na}_{5/6}\text{Li}_{5/18}\text{Mn}_{13/18}\text{O}_2$ (see Table S15-17 for details). (D) Schematic illustration of the corresponding structure with the Li/Mn ordering in the $[\text{Li}_{5/18}\text{Mn}_{13/18}]\text{O}_2$ slabs.

We then use cationic potential to design a P2-type structure aiming at an anomalous high Na-content of $x > 0.67$, again starting from $\text{NaLi}_{1/3}\text{Mn}_{2/3}\text{O}_2$. To avoid formation of O3-type structure, the dividing line in Fig. 1B demonstrates that we should increase the cationic potential (Eq.1), assuming that Na content remains constant, which can be realized by increasing the ionic potential at TM sites. Based on the cationic potential, a P2-type structure with $x=1$ ($\overline{\Phi}_{Na} = 9.8$) will demand an extremely large TM ionic potential (larger than that of Mn^{4+} , having the largest value among the widely used TMs). Therefore, the Na content in $\text{NaLi}_{1/3}\text{Mn}_{2/3}\text{O}_2$ should be lowered, which can be achieved through charge compensation by decreasing the Li and increasing the Mn content. Following this route, the cationic potential predicts that high Na-content $\text{Na}_{5/6}\text{Li}_{5/18}\text{Mn}_{13/18}\text{O}_2$ composition should have the P2-type structure (Fig. 3A), which was indeed successfully prepared (Fig. 3B). So far, layered oxides prepared with such high Na content usually crystallize as O3-type structure. Compared to the O3-type $\text{NaLi}_{1/3}\text{Ti}_{1/6}\text{Mn}_{1/2}\text{O}_2$, the (002) peak of P2-type structure shifts towards lower diffraction angles, indicating that the expected increase in the c -axis of the unit cell (Fig. 3B). Rietveld refinement of the XRD pattern reveals that this P2-type layered structure can be indexed in the hexagonal $P6_3$ space group (Fig. 3C, D). The electron energy loss spectroscopy mapping reveals a uniform distribution of the Na, Mn, and O elements in the plate-like particles (Fig. S11). Importantly, this as-prepared high Na-content material has significantly higher capacity of >200 mAh g^{-1} (Fig. S10B).

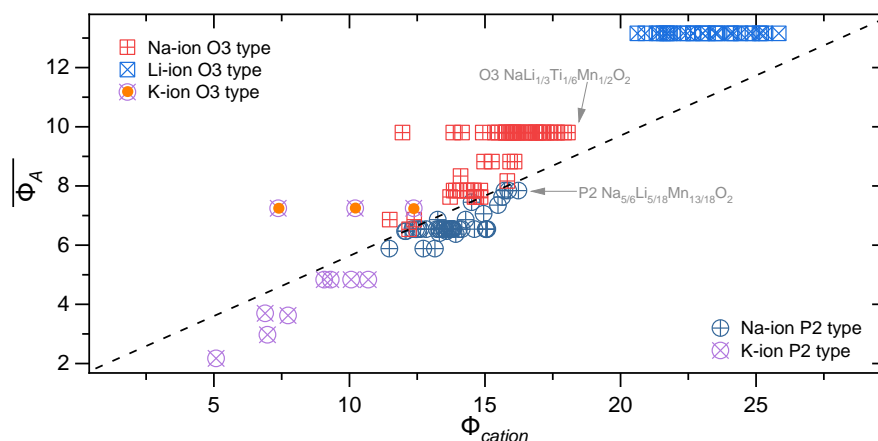


Fig. 4. Cationic potential phase map for layered alkali metal oxides. Summary of reported layered alkali metal materials including Li-/Na-/K-ion oxides (see Table S18 and S19 for details).

Extending the cationic potential to other alkali metal layered oxides, Li-ion (Fig. S12) and K-ion (Fig. S13), results in phase maps shown in Fig. 4. The cationic potential (Eq. 1), is found to increase from K- to Na- to Li-ion owing to the increasing ability to shield the TMO₂ interslab interaction. As a consequence, K_xTMO₂ mainly crystallizes as P2-type and Li_xTMO₂ as the O3-type structure, whereas Na_xTMO₂ is the most interesting family as the shielding strength is at the tipping point between P2- and O3-type structures. The distribution of reported layered electrodes exhibits a clear trend by clustering around the dividing line (Fig. 4). For more than 100,000 new compositions, up to quaternary compositions on the TM position, the cationic potential is used to predict the most stable stacking structure, resulting in a distribution of compositions in the phase map around the dividing line (see Fig. S14, S15, and supplementary text for details). This demonstrates how the cationic potential can be used to predict the structure of new Na_xTMO₂ layered materials, based on specific compositional demands. It is worth noting that the other parts far away from the line may also lead to other types of TM-oxide phases (e.g., rocksalt, spinel, etc.), or may not lead to stable structures at all, which is subject of ongoing investigations.

In summary, the ionic potential is a measure of the polarization of ions, mainly reflecting the influence of electrostatic energy on the system. Since the main difference between P- and O-type structures is the electrostatic polarization between AO₂ (A = alkali metals) and TMO₂ slabs, we can apply the proposed cationic potential method to distinguish and design materials, especially useful for Na-ion layered oxides. It should be noted that for entropy dominated phases, disordered compounds resulting from mechanical milling(20), or oxides prepared under particular conditions(21, 22), metastable structures or non-equilibrium phases(23), as well as the local distortion of TMs (e.g., due to Jahn-Teller effect on Mn³⁺), the ionic potential approach does not provide a sensible guideline. Moreover, the cationic potential only predicts if the proposed material will crystallize in P- or O-type structure, and one composition has only one structure. Because the actual obtained phases depend strongly on the nature of precursors and the conditions/atmosphere of thermal treatment, etc., which may cause the difference in stoichiometry and dynamic process, leading to structural changes. Further structural information is required to decide whether the corresponding material is stable/synthesizable in practice and calls for extensive investigation. Additionally, prediction of stacking structures is rather challenging for density functional theory

methods because the difficulty to predict the localized nature of TM orbitals, and especially for complicated TM compositions that have an enormous configurational space. We demonstrated the use of ionic potentials to tune the TMO_2 interslab interaction, contributing to the important categories of layered materials. The currently known layered materials are either low Na-content ($x=2/3$) P2-type oxides or high Na-content ($x=1$) O3-type oxides, we suggest further exploration of high Na-content P2-type oxides and low Na-content O3-type oxides through the as-proposed cationic potential.

References and Notes:

1. B. Dunn, H. Kamath, J.-M. Tarascon, Electrical Energy Storage for the Grid: A Battery of Choices. *Science* **334**, 928 (2011).
2. S.-W. Kim, D.-H. Seo, X. Ma, G. Ceder, K. Kang, Electrode Materials for Rechargeable Sodium-Ion Batteries: Potential Alternatives to Current Lithium-Ion Batteries. *Adv. Energy Mater.* **2**, 710-721 (2012).
3. M. H. Han, E. Gonzalo, G. Singh, T. Rojo, A comprehensive review of sodium layered oxides: powerful cathodes for Na-ion batteries. *Energy Environ. Sci.* **8**, 81-102 (2015).
4. K. Mizushima, P. C. Jones, P. J. Wiseman, J. B. Goodenough, Li_xCoO_2 ($0 < x < 1$): A new cathode material for batteries of high energy density. *Mater. Res. Bull.* **15**, 783-789 (1980).
5. N. Yabuuchi *et al.*, P2-type $\text{Na}_x[\text{Fe}_{1/2}\text{Mn}_{1/2}]\text{O}_2$ made from earth-abundant elements for rechargeable Na batteries. *Nat. Mater.* **11**, 512 (2012).
6. C. Delmas, C. Fouassier, P. Hagenmuller, Structural classification and properties of the layered oxides. *Phys. B+C* **99**, 81-85 (1980).
7. C. Fouassier, C. Delmas, P. Hagenmuller, Evolution structurale et proprietes physiques des phases A_xMO_2 ($\text{A} = \text{Na}, \text{K}; \text{M} = \text{Cr}, \text{Mn}, \text{Co}$) ($x \leq 1$). *Mater. Res. Bull.* **10**, 443-449 (1975).
8. S. Komaba *et al.*, Study on the Reversible Electrode Reaction of $\text{Na}_{1-x}\text{Ni}_{0.5}\text{Mn}_{0.5}\text{O}_2$ for a Rechargeable Sodium-Ion Battery. *Inorg. Chem.* **51**, 6211-6220 (2012).
9. J. M. Paulsen, R. A. Donabarger, J. R. Dahn, Layered T2-, O6-, O2-, and P2-Type $\text{A}_{2/3}[\text{M}^{2+}_{1/3}\text{M}^{4+}_{2/3}]\text{O}_2$ Bronzes, $\text{A} = \text{Li}, \text{Na}; \text{M}' = \text{Ni}, \text{Mg}; \text{M} = \text{Mn}, \text{Ti}$. *Chem. Mater.* **12**, 2257-2267 (2000).
10. J. Billaud *et al.*, $\text{Na}_{0.67}\text{Mn}_{1-x}\text{Mg}_x\text{O}_2$ ($0 \leq x \leq 0.2$): a high capacity cathode for sodium-ion batteries. *Energy Environ. Sci.* **7**, 1387-1391 (2014).
11. M. Guilmard, L. Croguennec, C. Delmas, Effects of Manganese Substitution for Nickel on the Structural and Electrochemical Properties of LiNiO_2 . *J. Power Sources* **150**, A1287-A1293 (2003).
12. C. Zhao, M. Avdeev, L. Chen, Y.-S. Hu, An O3-type Oxide with Low Sodium Content as the Phase-Transition-Free Anode for Sodium-Ion Batteries. *Angew. Chem. Int. Ed.* **57**, 7056-7060 (2018).
13. G. H. Cartledge, STUDIES ON THE PERIODIC SYSTEM. I. THE IONIC POTENTIAL AS A PERIODIC FUNCTION1. *J. Am. Chem. Soc.* **50**, 2855-2863 (1928).
14. C. Delmas, J.-J. Braconnier, C. Fouassier, P. Hagenmuller, Electrochemical intercalation of sodium in Na_xCoO_2 bronzes. *Solid State Ionics* **3-4**, 165-169 (1981).
15. Y.-J. Shin, M.-Y. Yi, Preparation and structural properties of layer-type oxides $\text{Na}_x\text{Ni}_{x/2}\text{Ti}_{1-x/2}\text{O}_2$ ($0.60 \leq x \leq 1.0$). *Solid State Ionics* **132**, 131-141 (2000).
16. G. Singh *et al.*, High Voltage Mg-Doped $\text{Na}_{0.67}\text{Ni}_{0.3-x}\text{Mg}_x\text{Mn}_{0.7}\text{O}_2$ ($x = 0.05, 0.1$) Na-Ion Cathodes with Enhanced Stability and Rate Capability. *Chem. Mater.* **28**, 5087-5094 (2016).
17. C. Delmas, C. Fouassier, P. Hagenmuller, Stabilité relative des environnements octaédrique et prismatique triangulaire dans les oxydes lamellaires alcalins A_xMO_2 ($x \leq 1$). *Mater. Res. Bull.* **11**, 1483-1488 (1976).
18. J. Rouxel, Sur un diagramme ionicité-structure pour les composés intercalaires alcalins des sulfures lamellaires. *J. Solid State Chem.* **17**, 223-229 (1976).
19. D. Kim, M. Cho, K. Cho, Rational Design of $\text{Na}(\text{Li}_{1/3}\text{Mn}_{2/3})\text{O}_2$ Operated by Anionic Redox Reactions for Advanced Sodium-Ion Batteries. *Adv. Mater.* **29**, 1701788 (2017).

20. T. Sato, K. Sato, W. Zhao, Y. Kajiya, N. Yabuuchi, Metastable and nanosize cation-disordered rocksalt-type oxides: revisit of stoichiometric LiMnO_2 and NaMnO_2 . *J. Mater. Chem. A* **6**, 13943-13951 (2018).
21. T. Uyama, K. Mukai, I. Yamada, Synthesis of Rhombohedral $\text{LiCo}_{0.64}\text{Mn}_{0.36}\text{O}_2$ Using a High-Pressure Method. *Inorg. Chem.* **58**, 6684-6695 (2019).
22. M. H. Han *et al.*, Synthesis and Electrochemistry Study of P2- and O3-phase $\text{Na}_{2/3}\text{Fe}_{1/2}\text{Mn}_{1/2}\text{O}_2$. *Electrochim. Acta* **182**, 1029-1036 (2015).
23. M. Bianchini *et al.*, The interplay between thermodynamics and kinetics in the solid-state synthesis of layered oxides. *Nature Materials*, (2020), doi.org/10.1038/s41563-020-0688-6.
24. S. C. Vogel, gsaslanguage: a GSAS script language for automated Rietveld refinements of diffraction data. *J. Appl. Crystallog.* **44**, 873-877 (2011).
25. C. Delmas, C. Fouassier, P. Hagenmuller, Structural classification and properties of the layered oxides. *Physica B+C* **99**, 81-85 (1980).
26. M. M. Claude Delmas, C. Fouassier, P. Hagenmuller, Stabilité relative des environnements octaédrique et prismatique triangulaire dans les oxydes lamellaires alcalins A_xMO_2 ($x \leq 1$). *Mater. Res. Bull.* **11**, 1483-1488 (1976).
27. J. Rouxel, Sur un diagramme ionicité-structure pour les composés intercalaires alcalins des sulfures lamellaires. *J. Solid State Chem.* **17**, 223-229 (1976).
28. L. Pauling, The Nature of the Chemical Bond, 3rd Edition. *The Nature of the Chemical Bond, 3rd Edition, Cornell University Press, Ithaca*, (1960).
29. J. R. Croy *et al.*, First-Cycle Evolution of Local Structure in Electrochemically Activated Li_2MnO_3 . *Chem. Mater.* **26**, 7091-7098 (2014).
30. H. Watanabe, M. Fukase, Weak Ferromagnetism in $\beta\text{-NaFeO}_2$. *J. Phys. Soc. Japan* **16**, 1181-1184 (1961).
31. R. Hoppe, H. Sabrowsky, Oxoscandate der Alkalimetalle: KScO_2 und RbScO_2 . *Zeitschrift für anorganische und allgemeine Chemie* **339**, 144-154 (1965).
32. N. Zafar Ali, J. Nuss, M. Jansen, A New Polymorph of Potassium Chromate(III), $\beta\text{-KCrO}_2$, and Reinvestigation of $\alpha\text{-KCrO}_2$. *Zeitschrift für anorganische und allgemeine Chemie* **639**, 241-245 (2013).
33. C. Delmas, M. Devalette, C. Fouassier, P. Hagenmuller, Les phases K_xCrO_2 ($x \leq 1$). *Mater. Res. Bull.* **10**, 393-398 (1975).
34. E. Gonzalo *et al.*, Synthesis and characterization of pure P2- and O3- $\text{Na}_{2/3}\text{Fe}_{2/3}\text{Mn}_{1/3}\text{O}_2$ as cathode materials for Na ion batteries. *J. Mater. Chem. A* **2**, 18523-18530 (2014).
35. M. H. Han *et al.*, Synthesis and Electrochemistry Study of P2- and O3-phase $\text{Na}_{2/3}\text{Fe}_{1/2}\text{Mn}_{1/2}\text{O}_2$. *Electrochim. Acta* **182**, 1029-1036 (2015).
36. E. Watanabe *et al.*, Redox-Driven Spin Transition in a Layered Battery Cathode Material. *Chem. Mater.* **31**, 2358-2365 (2019).
37. L. Bordet-Le Guenne, P. Deniard, P. Biensan, C. Siret, R. Brec, Structural study of two layered phases in the $\text{Na}_x\text{Mn}_y\text{O}_2$ system. Electrochemical behavior of their lithium substituted derivatives. *J. Mater. Chem.* **10**, 2201-2206 (2000).
38. Y. Ono, N. Kato, Y. Ishii, Y. Miyazaki, T. Kajitani, Crystal Structure and Transport Properties of gamma; Na_xCoO_2 ($x=0.67-0.75$). *J. Japan Soc. Powder Powder Metal.* **50**, 469-474 (2003).

39. J. M. Paulsen, R. A. Donaberger, J. R. Dahn, Layered T2-, O6-, O2-, and P2-Type $A_{2/3}[M^{2+}_{1/3}M^{4+}_{2/3}]O_2$ Bronzes, A = Li, Na; M' = Ni, Mg; M = Mn, Ti. *Chem. Mater.* **12**, 2257-2267 (2000).
40. T. Zhou, D. Zhang, T. W. Button, F. J. Berry, C. Greaves, Substitution effects on the structural and magnetic behaviour of $Na_{0.63}CoO_2$. *Dalton Trans.* **39**, 1089-1094 (2010).
41. O. A. Smirnova, M. Avdeev, V. B. Nalbandyan, V. V. Kharton, F. M. B. Marques, First observation of the reversible O3 \leftrightarrow P2 phase transition: Crystal structure of the quenched high-temperature phase $Na_{0.74}Ni_{0.58}Sb_{0.42}O_2$. *Mater. Res. Bull.* **41**, 1056-1062 (2006).
42. Y.-J. Shin, M.-Y. Yi, Preparation and structural properties of layer-type oxides $Na_xNi_{x/2}Ti_{1-x/2}O_2$ ($0.60 \leq x \leq 1.0$). *Solid State Ionics* **132**, 131-141 (2000).
43. Y.-J. Shin, M.-H. Park, J.-H. Kwak, H. Namgoong, O. H. Han, Ionic conduction properties of layer-type oxides $Na_xM_{x/2}^{II}Ti_{1-x/2}^{IV}O_2$ (M=Ni, Co; $0.60 \leq x \leq 1.0$). *Solid State Ionics* **150**, 363-372 (2002).
44. G. V. Shilov, V. B. Nalbandyan, V. A. Volochaev, L. O. Atovmyan, Crystal growth and crystal structures of the layered ionic conductors–sodium lithium titanium oxides. *Int. J. Inorg. Mater.* **2**, 443-449 (2000).
45. J.S. J. Clarke, A. J. Fowkes, A. Harrison, R. M. Ibberson, M. J. Rosseinsky, Synthesis, Structure, and Magnetic Properties of $NaTiO_2$. *Chem. Mater.* **10**, 372-384 (1998).
46. S. J. Clarke, A. J. Fowkes, A. Harrison, R. M. Ibberson, M. J. Rosseinsky, Synthesis, Structure, and Magnetic Properties of $NaTiO_2$. *Chemistry of Materials* **10**, 372-384 (1998).
47. W. Scheld, R. Hoppe, Über den α - $NaFeO_2$ -Typ: Zur Kenntnis von $NaCrO_2$ und $KCrO_2$. *Zeitschrift für anorganische und allgemeine Chemie* **568**, 151-156 (1989).
48. C. Fouassier, G. Matejka, J.-M. Reau, P. Hagemuller, Sur de nouveaux bronzes oxygénés de formule Na_xCoO_2 . Le système cobalt-oxygène-sodium. *J. Solid State Chem.* **6**, 532-537 (1973).
49. J. Bréger, K. Kang, J. Cabana, G. Ceder, C. P. Grey, NMR, PDF and RMC study of the positive electrode material $Li(Ni_{0.5}Mn_{0.5})O_2$ synthesized by ion-exchange methods. *J. Mater. Chem.* **17**, 3167-3174 (2007).
50. P. Vassilaras, A. J. Toumar, G. Ceder, Electrochemical properties of $NaNi_{1/3}Co_{1/3}Fe_{1/3}O_2$ as a cathode material for Na-ion batteries. *Electrochem. Commun.* **38**, 79-81 (2014).
51. S.-M. Oh *et al.*, Advanced $Na[Ni_{0.25}Fe_{0.5}Mn_{0.25}]O_2/C-Fe_3O_4$ Sodium-Ion Batteries Using EMS Electrolyte for Energy Storage. *Nano Letters* **14**, 1620-1626 (2014).
52. C. Zhao, M. Avdeev, L. Chen, Y.-S. Hu, An O3-type Oxide with Low Sodium Content as the Phase-Transition-Free Anode for Sodium-Ion Batteries. *Angew. Chem. Int. Ed.* **57**, 7056-7060 (2018).
53. R. D. Shannon, Revised effective ionic radii and systematic studies of interatomic distances in halides and chalcogenides. *Acta Crystallographica Section A* **32**, 751-767 (1976).
54. A. Caballero *et al.*, Synthesis and characterization of high-temperature hexagonal P2- $Na_{0.6}MnO_2$ and its electrochemical behaviour as cathode in sodium cells. *J. Mater. Chem.* **12**, 1142-1147 (2002).
55. Y. Wang, R. Xiao, Y.-S. Hu, M. Avdeev, L. Chen, P2- $Na_{0.6}[Cr_{0.6}Ti_{0.4}]O_2$ cation-disordered electrode for high-rate symmetric rechargeable sodium-ion batteries. *Nat. Commun.* **6**, 6954 (2015).
56. N.-A. Nguyen *et al.*, Effect of Calcination Temperature on a P-type $Na_{0.6}Mn_{0.65}Ni_{0.25}Co_{0.10}O_2$ Cathode Material for Sodium-Ion Batteries. *J. Electrochem. Soc.* **164**, A6308-A6314 (2017).

57. T.-Y. Yu, J.-Y. Hwang, D. Aurbach, Y.-K. Sun, Microsphere $\text{Na}_{0.65}[\text{Ni}_{0.17}\text{Co}_{0.11}\text{Mn}_{0.72}]\text{O}_2$ Cathode Material for High-Performance Sodium-Ion Batteries. *ACS Appl. Mater. Inter.* **9**, 44534-44541 (2017).
58. C. Zhao *et al.*, Decreasing transition metal triggered oxygen redox activity in Na-deficient oxides. *Energy Storage Mater.*, **20**, 395–400 (2018).
59. X. Cao *et al.*, Stabilizing Reversible Oxygen Redox Chemistry in Layered Oxides for Sodium-Ion Batteries. *Adv. Energy Mater.* **10**, 1903785 (2020).
60. A. P. Tyutyunnik *et al.*, Synthesis, Superconducting Properties and Structural (Including Electron Diffraction) Studies of Na_xNbO_2 and Li_xNbO_2 . *ChemInform* **27**, (1996).
61. Z.-Y. Li, R. Gao, L. Sun, Z. Hu, X. Liu, Designing an advanced P2- $\text{Na}_{0.67}\text{Mn}_{0.65}\text{Ni}_{0.2}\text{Co}_{0.15}\text{O}_2$ layered cathode material for Na-ion batteries. *J. Mater. Chem. A* **3**, 16272-16278 (2015).
62. M. Valvo, S. Doubaji, I. Saadoune, K. Edström, Pseudocapacitive charge storage properties of $\text{Na}_{2/3}\text{Co}_{2/3}\text{Mn}_{2/9}\text{Ni}_{1/9}\text{O}_2$ in Na-ion batteries. *Electrochim. Acta* **276**, 142-152 (2018).
63. Y. Wang, J. Tang, X. Yang, W. Huang, A study on electrochemical properties of P2-type Na–Mn–Co–Cr–O cathodes for sodium-ion batteries. *Inorg. Chem. Front.* **5**, 577-584 (2018).
64. D. Su, C. Wang, H.-j. Ahn, G. Wang, Single Crystalline $\text{Na}_{0.7}\text{MnO}_2$ Nanoplates as Cathode Materials for Sodium-Ion Batteries with Enhanced Performance. *Chem. A Eur. J.* **19**, 10884-10889 (2013).
65. N. Yabuuchi *et al.*, A new electrode material for rechargeable sodium batteries: P2-type $\text{Na}_{2/3}[\text{Mg}_{0.28}\text{Mn}_{0.72}]\text{O}_2$ with anomalously high reversible capacity. *J. Mater. Chem. A* **2**, 16851-16855 (2014).
66. X. Bai *et al.*, Anionic Redox Activity in a Newly Zn-Doped Sodium Layered Oxide P2- $\text{Na}_{2/3}\text{Mn}_{1-y}\text{Zn}_y\text{O}_2$ ($0 < y < 0.23$). *Adv. Energy Mater.* **8**, 1802379 (2018).
67. N. Hamada, T. Imai, H. Funashima, Thermoelectric power calculation by the Boltzmann equation: Na_xCoO_2 . *J. Phys. Condens. Mat.* **19**, 365221 (2007).
68. Y.-E. Zhu *et al.*, A P2- $\text{Na}_{0.67}\text{Co}_{0.5}\text{Mn}_{0.5}\text{O}_2$ cathode material with excellent rate capability and cycling stability for sodium ion batteries. *J. Mater. Chem. A* **4**, 11103-11109 (2016).
69. Y. Wang *et al.*, A zero-strain layered metal oxide as the negative electrode for long-life sodium-ion batteries. *Nat. Commun.* **4**, 2365 (2013).
70. H. Hou, B. Gan, Y. Gong, N. Chen, C. Sun, P2-Type $\text{Na}_{0.67}\text{Ni}_{0.23}\text{Mg}_{0.1}\text{Mn}_{0.67}\text{O}_2$ as a High-Performance Cathode for a Sodium-Ion Battery. *Inorg. Chem.* **55**, 9033-9037 (2016).
71. L. Wang *et al.*, Copper-substituted $\text{Na}_{0.67}\text{Ni}_{0.3-x}\text{Cu}_x\text{Mn}_{0.7}\text{O}_2$ cathode materials for sodium-ion batteries with suppressed P2–O2 phase transition. *J. Mater. Chem. A* **5**, 8752-8761 (2017).
72. X. Wu *et al.*, P2-type $\text{Na}_{0.66}\text{Ni}_{0.33-x}\text{Zn}_x\text{Mn}_{0.67}\text{O}_2$ as new high-voltage cathode materials for sodium-ion batteries. *J. Power Sour.* **281**, 18-26 (2015).
73. H. Yoshida *et al.*, P2-type $\text{Na}_{2/3}\text{Ni}_{1/3}\text{Mn}_{2/3-x}\text{Ti}_x\text{O}_2$ as a new positive electrode for higher energy Na-ion batteries. *Chem. Commun.* **50**, 3677-3680 (2014).
74. L. Mu *et al.*, Water-Processable P2- $\text{Na}_{0.67}\text{Ni}_{0.22}\text{Cu}_{0.11}\text{Mn}_{0.56}\text{Ti}_{0.11}\text{O}_2$ Cathode Material for Sodium Ion Batteries. *J. Electrochem. Soc.* **166**, A251-A257 (2019).
75. T. Matsumura, N. Sonoyama, R. Kanno, Synthesis, structure and electrochemical properties of layered material, $\text{Li}_{2/3}[\text{Mn}_{1/3}\text{Fe}_{2/3}]\text{O}_2$, with mixed stacking states. *Solid State Ionics* **161**, 31-39 (2003).

76. W. M. Dose *et al.*, Structure–Electrochemical Evolution of a Mn-Rich P2 Na_{2/3}Fe_{0.2}Mn_{0.8}O₂ Na-Ion Battery Cathode. *Chem. Mater.* **29**, 7416-7423 (2017).
77. M. H. Han *et al.*, High-Performance P2-Phase Na_{2/3}Mn_{0.8}Fe_{0.1}Ti_{0.1}O₂ Cathode Material for Ambient-Temperature Sodium-Ion Batteries. *Chem. Mater.* **28**, 106-116 (2016).
78. C. Luo, A. Langrock, X. Fan, Y. Liang, C. Wang, P2-type transition metal oxides for high performance Na-ion battery cathodes. *J. Mater. Chem. A* **5**, 18214-18220 (2017).
79. L. Liu *et al.*, High-Performance P2-Type Na_{2/3}(Mn_{1/2}Fe_{1/4}Co_{1/4})O₂ Cathode Material with Superior Rate Capability for Na-Ion Batteries. *Adv. Energy Mater.* **5**, 1500944 (2015).
80. K. Kaliyappan, J. Liu, A. Lushington, R. Li, X. Sun, Highly Stable Na_{2/3}(Mn_{0.54}Ni_{0.13}Co_{0.13})O₂ Cathode Modified by Atomic Layer Deposition for Sodium-Ion Batteries. *ChemSusChem* **8**, 2537-2543 (2015).
81. X. Sun *et al.*, Sodium insertion cathode material Na_{0.67}[Ni_{0.4}Co_{0.2}Mn_{0.4}]O₂ with excellent electrochemical properties. *Electrochim. Acta* **208**, 142-147 (2016).
82. Y. Tsuchiya *et al.*, Layered Na_xCr_xTi_{1-x}O₂ as Bifunctional Electrode Materials for Rechargeable Sodium Batteries. *Chem. Mater.* **28**, 7006-7016 (2016).
83. M. A. Evstigneeva, V. B. Nalbandyan, A. A. Petrenko, B. S. Medvedev, A. A. Kataev, A New Family of Fast Sodium Ion Conductors: Na₂M₂TeO₆ (M = Ni, Co, Zn, Mg). *Chem. Mater.* **23**, 1174-1181 (2011).
84. J. Yoshida *et al.*, New P2-Na_{0.70}Mn_{0.60}Ni_{0.30}Co_{0.10}O₂ Layered Oxide as Electrode Material for Na-Ion Batteries. *J. Electrochem. Soc.* **161**, A1987-A1991 (2014).
85. X. Rong *et al.*, Anionic Redox Reaction-Induced High-Capacity and Low-Strain Cathode with Suppressed Phase Transition. *Joule*, **3**, 503-517 (2018).
86. Q. Huang, J. W. Lynn, B. H. Toby, M. L. Foo, R. J. Cava, Characterization of the structural transition in Na_{0.75}CoO₂. *J. Phys. Condens. Mat.* **17**, 1831-1840 (2005).
87. R. J. Balsys, R. Lindsay Davis, Refinement of the structure of Na_{0.74}CoO₂ using neutron powder diffraction. *Solid State Ionics* **93**, 279-282 (1997).
88. Y. Li *et al.*, Air-Stable Copper-Based P2-Na_{7/9}Cu_{2/9}Fe_{1/9}Mn_{2/3}O₂ as a New Positive Electrode Material for Sodium-Ion Batteries. *Adv. Sci.* **2**, 1500031 (2015).
89. X. Qi, Layered Oxide Cathode Materials for Sodium-Ion Batteries and the Industrial Exploration. *University of Chinese Academy of Sciences*, (2018).
90. R. J. Clément *et al.*, Direct evidence for high Na⁺ mobility and high voltage structural processes in P2-Na_x[Li_yNi_zMn_{1-y-z}]O₂ (x, y, z ≤ 1) cathodes from solid-state NMR and DFT calculations. *J. Mater. Chem. A* **5**, 4129-4143 (2017).
91. D. Wu *et al.*, NaTiO₂: a layered anode material for sodium-ion batteries. *Energy Environ. Sci.* **8**, 195-202 (2015).
92. B. L. Chamberland, S. K. Porter, A study on the preparation and physical property determination of NaVO₂. *J. Solid State Chem.* **73**, 398-404 (1988).
93. X. Xia, J. R. Dahn, NaCrO₂ is a Fundamentally Safe Positive Electrode Material for Sodium-Ion Batteries with Liquid Electrolytes. *Electrochem. Solid-State Lett.* **15**, A1-A4 (2012).
94. Y. Takeda, J. Akagi, A. Edagawa, M. Inagaki, S. Naka, A preparation and polymorphic relations of sodium iron oxide (NaFeO₂). *Mater. Res. Bull.* **15**, 1167-1172 (1980).
95. C. Ringenbach, H. Kessler, A. C. R. Khatteer, Chimie Minerale.-Un nouveau compose oxygene du molybdene NaMoO₂. Proprietes cristallographiques et magnetiques. *C. R. Seances Acad. Sci., Ser. C* **269**, 1394 (1969).

96. K. Hobbie, R. Hoppe, Zum Aufbau von NaRhO₂. *Zeitschrift für anorganische und allgemeine Chemie* **565**, 106-110 (1988).
97. G. Blasse, Sodium lanthanide oxides NaLnO₂. *J. Inorg. Nuclear Chem.* **28**, 2444-2445 (1966).
98. H. Yoshida, N. Yabuuchi, S. Komaba, NaFe_{0.5}Co_{0.5}O₂ as high energy and power positive electrode for Na-ion batteries. *Electrochem. Commun.* **34**, 60-63 (2013).
99. S. Song *et al.*, Y-Doped Na₂ZrO₃: A Na-Rich Layered Oxide as a High-Capacity Cathode Material for Sodium-Ion Batteries. *ACS Sustain. Chem. Eng.* **5**, 4785-4792 (2017).
100. K. M. Mogare, K. Friese, W. Klein, M. Jansen, Syntheses and Crystal Structures of Two Sodium Ruthenates: Na₂RuO₄ and Na₂RuO₃. *Zeitschrift für anorganische und allgemeine Chemie* **630**, 547-552 (2004).
101. R. V. Panin *et al.*, Synthesis and crystal structure of the palladium oxides NaPd₃O₄, Na₂PdO₃ and K₃Pd₂O₄. *J. Solid State Chem.* **180**, 1566-1574 (2007).
102. A. J. Perez *et al.*, Strong Oxygen Participation in the Redox Governing the Structural and Electrochemical Properties of Na-Rich Layered Oxide Na₂IrO₃. *Chem. Mater.* **28**, 8278-8288 (2016).
103. C. L. McDaniel, Phase relations in the systems Na₂O-IrO₂ and Na₂O-PtO₂ in air. *J. Solid State Chem.* **9**, 139-146 (1974).
104. S. Liu *et al.*, Na₂Ru_{0.8}Mn_{0.2}O₃: A novel cathode material for ultrafast sodium ion battery with large capacity and superlong cycle life. *J. Power Sour.* **421**, 14-22 (2019).
105. P. Rozier *et al.*, Anionic redox chemistry in Na-rich Na₂Ru_{1-y}Sn_yO₃ positive electrode material for Na-ion batteries. *Electrochem. Commun.* **53**, 29-32 (2015).
106. N. Su, Y. Lyu, B. Guo, Electrochemical and in-situ X-ray diffraction studies of Na_{1.2}Ni_{0.2}Mn_{0.2}Ru_{0.4}O₂ as a cathode material for sodium-ion batteries. *Electrochem. Commun.* **87**, 71-75 (2018).
107. K. A. Regan, Q. Huang, R. J. Cava, Isolated spin 3/2 plaquettes in Na₃RuO₄. *J. Solid State Chem.* **178**, 2104-2108 (2005).
108. Y. Qiao *et al.*, Reversible anionic redox activity in Na₃RuO₄ cathodes: a prototype Na-rich layered oxide. *Energy Environ. Sci.* **11**, 299-305 (2018).
109. C. Wang *et al.*, The top-down synthesis of sequentially controlled architectures for honeycomb-layered Na₃Ni₂BiO₆ towards high-voltage and superior performance cathodes for sodium-ion batteries. *J. Mater. Chem. A* **7**, 1797-1809 (2019).
110. J. Ma *et al.*, Ordered and Disordered Polymorphs of Na(Ni_{2/3}Sb_{1/3})O₂: Honeycomb-Ordered Cathodes for Na-Ion Batteries. *Chem. Mater.* **27**, 2387-2399 (2015).
111. Q. Li *et al.*, A Superlattice-Stabilized Layered Oxide Cathode for Sodium-Ion Batteries. *Adv. Mater.* **32**, 1907936 (2020).
112. O. A. Smirnova, V. B. Nalbandyan, A. A. Petrenko, M. Avdeev, Subsolidus phase relations in Na₂O-CuO-Sb₂O_n system and crystal structure of new sodium copper antimonate Na₃Cu₂SbO₆. *J. Solid State Chem.* **178**, 1165-1170 (2005).
113. M.-H. Cao *et al.*, Suppressing the chromium disproportionation reaction in O3-type layered cathode materials for high capacity sodium-ion batteries. *J. Mater. Chem. A* **5**, 5442-5448 (2017).
114. X. Chen *et al.*, Reversible Flat to Rippling Phase Transition in Fe Containing Layered Battery Electrode Materials. *Adv. Funct. Mater.* **28**, 1803896 (2018).
115. D. Kim *et al.*, Layered Na[Ni_{1/3}Fe_{1/3}Mn_{1/3}]O₂ cathodes for Na-ion battery application. *Electrochem. Commun.* **18**, 66-69 (2012).

116. M. Sathiya, K. Hemalatha, K. Ramesha, J. M. Tarascon, A. S. Prakash, Synthesis, Structure, and Electrochemical Properties of the Layered Sodium Insertion Cathode Material: $\text{NaNi}_{1/3}\text{Mn}_{1/3}\text{Co}_{1/3}\text{O}_2$. *Chem. Mater.* **24**, 1846-1853 (2012).
117. H. Xu *et al.*, Synthesis and evaluation of $\text{NaNi}_{0.5}\text{Co}_{0.2}\text{Mn}_{0.3}\text{O}_2$ as a cathode material for Na-ion battery. *Ceram. Int.* **42**, 12521-12524 (2016).
118. X. Li *et al.*, O3-type $\text{Na}(\text{Mn}_{0.25}\text{Fe}_{0.25}\text{Co}_{0.25}\text{Ni}_{0.25})\text{O}_2$: A quaternary layered cathode compound for rechargeable Na ion batteries. *Electrochem. Commun.* **49**, 51-54 (2014).
119. J.-Y. Hwang, S.-T. Myung, Y.-K. Sun, Quaternary Transition Metal Oxide Layered Framework: O3-Type $\text{Na}[\text{Ni}_{0.32}\text{Fe}_{0.13}\text{Co}_{0.15}\text{Mn}_{0.40}]\text{O}_2$ Cathode Material for High-Performance Sodium-Ion Batteries. *J. Phys. Chem. C* **122**, 13500-13507 (2018).
120. X. Sun *et al.*, $\text{Na}[\text{Ni}_{0.4}\text{Fe}_{0.2}\text{Mn}_{0.4-x}\text{Ti}_x]\text{O}_2$: a cathode of high capacity and superior cyclability for Na-ion batteries. *J. Mater. Chem. A* **2**, 17268-17271 (2014).
121. J.-L. Yue *et al.*, A quinary layer transition metal oxide of $\text{NaNi}_{1/4}\text{Co}_{1/4}\text{Fe}_{1/4}\text{Mn}_{1/8}\text{Ti}_{1/8}\text{O}_2$ as a high-rate-capability and long-cycle-life cathode material for rechargeable sodium ion batteries. *Chem. Commun.* **51**, 15712-15715 (2015).
122. J.-L. Yue *et al.*, O3-type layered transition metal oxide $\text{Na}(\text{NiCoFeTi})_{1/4}\text{O}_2$ as a high rate and long cycle life cathode material for sodium ion batteries. *J. Mater. Chem. A* **3**, 23261-23267 (2015).
123. S. Zhang *et al.*, O3-type $\text{NaNi}_{0.33}\text{Li}_{0.11}\text{Ti}_{0.56}\text{O}_2$ -based electrode for symmetric sodium ion cell. *J. Power Sour.* **329**, 1-7 (2016).
124. A. J. Perez, G. Rousse, J.-M. Tarascon, Structural Instability Driven by Li/Na Competition in $\text{Na}(\text{Li}_{1/3}\text{Ir}_{2/3})\text{O}_2$ Cathode Material for Li-Ion and Na-Ion Batteries. *Inorg. Chem.* **58**, 15644-15651 (2019).
125. X. Zhang *et al.*, Manganese-Based Na-Rich Materials Boost Anionic Redox in High-Performance Layered Cathodes for Sodium-Ion Batteries. *Adv. Mater.* **31**, 1807770 (2019).
126. H. Yu, S. Guo, Y. Zhu, M. Ishida, H. Zhou, Novel titanium-based O3-type $\text{NaTi}_{0.5}\text{Ni}_{0.5}\text{O}_2$ as a cathode material for sodium ion batteries. *Chem. Commun.* **50**, 457-459 (2014).
127. J. Wang *et al.*, O3-type $\text{Na}[\text{Fe}_{1/3}\text{Ni}_{1/3}\text{Ti}_{1/3}]\text{O}_2$ cathode material for rechargeable sodium ion batteries. *J. Mater. Chem. A* **4**, 3431-3437 (2016).
128. P.-F. Wang *et al.*, Ti-Substituted $\text{NaNi}_{0.5}\text{Mn}_{0.5-x}\text{Ti}_x\text{O}_2$ Cathodes with Reversible O3-P3 Phase Transition for High-Performance Sodium-Ion Batteries. *Adv. Mater.* **29**, 1700210 (2017).
129. H.-R. Yao *et al.*, Designing Air-Stable O3-Type Cathode Materials by Combined Structure Modulation for Na-Ion Batteries. *J. Am. Chem. Soc.* **139**, 8440-8443 (2017).
130. L. Mu *et al.*, Prototype Sodium-Ion Batteries Using an Air-Stable and Co/Ni-Free O3-Layered Metal Oxide Cathode. *Adv Mater* **27**, 6928-6933 (2015).
131. X. Li *et al.*, $\text{Na}_{0.9}\text{Ni}_{0.45}\text{Ti}_{0.55}\text{O}_2$ as novel bipolar material for sodium ion batteries. *Solid State Ionics* **334**, 14-20 (2019).
132. X. Qi *et al.*, Sodium-Deficient O3- $\text{Na}_{0.9}[\text{Ni}_{0.4}\text{Mn}_x\text{Ti}_{0.6-x}]\text{O}_2$ Layered-Oxide Cathode Materials for Sodium-Ion Batteries. *Part. Part. Syst. Char.* **33**, 538-544 (2016).
133. X. Jiang, F. Hu, J. Zhang, Sodium-deficient O3- $\text{Na}_{0.9}\text{Mn}_{0.4}\text{Fe}_{0.5}\text{Ti}_{0.1}\text{O}_2$ as a cathode material for sodium-ion batteries. *RSC Adv.* **6**, 103238-103241 (2016).
134. A. Varela, M. Parras, J. M. González-Calbet, Influence of Na Content on the Chemical Stability of Nanometric Layered Na_xRhO_2 ($0.7 \leq x \leq 1.0$). *Eur. J. Inorg. Chem.* **2005**, 4410-4416 (2005).

135. M.-H. Cao, Z. Shadik, Y.-N. Zhou, Z.-W. Fu, Sodium-deficient O3-type $\text{Na}_{0.83}\text{Cr}_{1/3}\text{Fe}_{1/3}\text{Mn}_{1/6}\text{Ti}_{1/6}\text{O}_2$ as a new cathode material for Na-ion batteries. *Electrochim. Acta* **295**, 918-925 (2019).
136. S. Guo *et al.*, High-performance symmetric sodium-ion batteries using a new, bipolar O3-type material, $\text{Na}_{0.8}\text{Ni}_{0.4}\text{Ti}_{0.6}\text{O}_2$. *Energy Environ. Sci.* **8**, 1237-1244 (2015).
137. H. Guo *et al.*, Na-deficient O3-type cathode material $\text{Na}_{0.8}[\text{Ni}_{0.3}\text{Co}_{0.2}\text{Ti}_{0.5}]\text{O}_2$ for room-temperature sodium-ion batteries. *Electrochim. Acta* **158**, 258-263 (2015).
138. J. S. Thorne, R. A. Dunlap, M. N. Obrovac, Structure and Electrochemistry of $\text{Na}_x\text{Fe}_x\text{Mn}_{1-x}\text{O}_2$ ($1.0 \leq x \leq 0.5$) for Na-Ion Battery Positive Electrodes. *J. Electrochem. Soc.* **160**, A361-A367 (2012).
139. O. A. Smirnova, J. Rocha, V. B. Nalbandyan, V. V. Kharton, F. M. B. Marques, Crystal structure, local sodium environments and ion dynamics in $\text{Na}_{0.8}\text{Ni}_{0.6}\text{Sb}_{0.4}\text{O}_2$, a new mixed antimonate. *Solid State Ionics* **178**, 1360-1365 (2007).
140. P.-F. Wang *et al.*, An Abnormal 3.7-Volt O3-Type Sodium-Ion Battery Cathode. *Angew. Chem. Int. Ed.* **57**, 8178-8183 (2018).
141. P.-F. Wang, H.-R. Yao, T.-T. Zuo, Y.-X. Yin, Y.-G. Guo, Novel P2-type $\text{Na}_{2/3}\text{Ni}_{1/6}\text{Mg}_{1/6}\text{Ti}_{2/3}\text{O}_2$ as an anode material for sodium-ion batteries. *Chem. Commun.* **53**, 1957-1960 (2017).
142. Castellanos, M., West, A.R. Order-disorder phenomena in oxides with rock salt structures: the system $\text{Li}_2\text{TiO}_3\text{-MgO}$. *J. Mater. Sci.* **14**, 450-454 (1979).
143. W. J. H. Borghols *et al.*, The electronic structure and ionic diffusion of nanoscale LiTiO_2 anatase. *Phys. Chem. Chem. Phys.* **11**, 5742-5748 (2009).
144. A. R. Armstrong, P. G. Bruce, Synthesis of layered LiMnO_2 as an electrode for rechargeable lithium batteries. *Nature* **381**, 499-500 (1996).
145. K. Ozawa, Lithium-ion rechargeable batteries with LiCoO_2 and carbon electrodes: the LiCoO_2/C system. *Solid State Ionics* **69**, 212-221 (1994).
146. K. Mukai, J. Sugiyama, Y. Aoki, Structural, magnetic, and electrochemical studies on lithium insertion materials $\text{LiNi}_{1-x}\text{Co}_x\text{O}_2$ with $0 \leq x \leq 0.25$. *J. Solid State Chem.* **183**, 1726-1732 (2010).
147. J. F. Dorrian, R. E. Newnham, Refinement of the structure of Li_2TiO_3 . *Mater. Res. Bull.* **4**, 179-183 (1969).
148. L. P. Cardoso, D. E. Cox, T. A. Hewston, B. L. Chamberland, Structural studies of $\text{Li}_{0.7}\text{VO}_2$ in the temperature range 20–300°C. *J. Solid State Chem.* **72**, 234-243 (1988).
149. S. Komaba, C. Takei, T. Nakayama, A. Ogata, N. Yabuuchi, Electrochemical intercalation activity of layered NaCrO_2 vs. LiCrO_2 . *Electrochem. Commun.* **12**, 355-358 (2010).
150. M. Jansen, R. Hoppe, Zur Kenntnis der NaCl-Strukturfamilie: Neue Untersuchungen an Li_2MnO_3 . *Zeitschrift für anorganische und allgemeine Chemie* **397**, 279-289 (1973).
151. Y. Lyu *et al.*, Probing Reversible Multielectron Transfer and Structure Evolution of $\text{Li}_{1.2}\text{Cr}_{0.4}\text{Mn}_{0.4}\text{O}_2$ Cathode Material for Li-Ion Batteries in a Voltage Range of 1.0–4.8 V. *Chem. Mater.* **27**, 5238-5252 (2015).
152. M. Gu *et al.*, Nanoscale Phase Separation, Cation Ordering, and Surface Chemistry in Pristine $\text{Li}_{1.2}\text{Ni}_{0.2}\text{Mn}_{0.6}\text{O}_2$ for Li-Ion Batteries. *Chem. Mater.* **25**, 2319-2326 (2013).
153. Y.-S. Hong, Y. J. Park, K. S. Ryu, S. H. Chang, Charge/discharge behavior of $\text{Li}[\text{Ni}_{0.20}\text{Li}_{0.20}\text{Mn}_{0.60}]\text{O}_2$ and $\text{Li}[\text{Co}_{0.20}\text{Li}_{0.27}\text{Mn}_{0.53}]\text{O}_2$ cathode materials in lithium secondary batteries. *Solid State Ionics* **176**, 1035-1042 (2005).

154. X. Yu *et al.*, Understanding the Rate Capability of High-Energy-Density Li-Rich Layered $\text{Li}_{1.2}\text{Ni}_{0.15}\text{Co}_{0.1}\text{Mn}_{0.55}\text{O}_2$ Cathode Materials. *Adv. Energy Mater.* **4**, 1300950 (2014).
155. H. Gwon *et al.*, Ion-Exchange Mechanism of Layered Transition-Metal Oxides: Case Study of $\text{LiNi}_{0.5}\text{Mn}_{0.5}\text{O}_2$. *Inorg. Chem.* **53**, 8083-8087 (2014).
156. M. V. Reddy, G. V. Subba Rao, B. V. R. Chowdari, Preparation and Characterization of $\text{LiNi}_{0.5}\text{Co}_{0.5}\text{O}_2$ and $\text{LiNi}_{0.5}\text{Co}_{0.4}\text{Al}_{0.1}\text{O}_2$ by Molten Salt Synthesis for Li Ion Batteries. *J. Phys. Chem. C* **111**, 11712-11720 (2007).
157. F. Ronci, B. Scrosati, V. R. Albertini, P. Perfetti, In Situ Energy Dispersive X-ray Diffraction Study of $\text{LiNi}_{0.8}\text{Co}_{0.2}\text{O}_2$ Cathode Material for Lithium Batteries. *J. Phys. Chem. B* **105**, 754-759 (2001).
158. V. B. Lazarev, I. S. Shaplygin, Electrical properties of mixed oxides containing platinum and base metals. *Zhurnal Neorganicheskoy Khimii* **23**, 291-303 (1978).
159. A. K. Kalathil, P. Arunkumar, D. H. Kim, J.-W. Lee, W. B. Im, Influence of Ti^{4+} on the Electrochemical Performance of Li-Rich Layered Oxides - High Power and Long Cycle Life of $\text{Li}_2\text{Ru}_{1-x}\text{Ti}_x\text{O}_3$ Cathodes. *ACS Appl. Mater. Inter.* **7**, 7118-7128 (2015).
160. M. Sathiya *et al.*, High Performance $\text{Li}_2\text{Ru}_{1-y}\text{Mn}_y\text{O}_3$ ($0.2 \leq y \leq 0.8$) Cathode Materials for Rechargeable Lithium-Ion Batteries: Their Understanding. *Chem. Mater.* **25**, 1121-1131 (2013).
161. Q. Jacquet *et al.*, Competition between Metal Dissolution and Gas Release in Li-Rich $\text{Li}_3\text{Ru}_y\text{Ir}_{1-y}\text{O}_4$ Model Compounds Showing Anionic Redox. *Chem. Mater.* **30**, 7682-7690 (2018).
162. W. Luo, X. Li, J. R. Dahn, Synthesis, Characterization, and Thermal Stability of $\text{Li}[\text{Ni}_{1/3}\text{Mn}_{1/3}\text{Co}_{1/3-z}(\text{MnMg})_{z/2}]\text{O}_2$. *Chem. Mater.* **22**, 5065-5073 (2010).
163. J. Jiang, K. W. Eberman, L. J. Krause, J. R. Dahn, Structure, Electrochemical Properties, and Thermal Stability Studies of $\text{Li}[\text{Ni}_{0.2}\text{Co}_{0.6}\text{Mn}_{0.2}]\text{O}_2$: Effect of Synthesis Route. *J. Electrochem. Soc.* **152**, A1874-A1878 (2005).
164. H. Arai, M. Tsuda, Y. Sakurai, Lithium nickelate electrodes with enhanced high-temperature performance and thermal stability. *J. Power Sour.* **90**, 76-81 (2000).
165. D. Mori *et al.*, Bulk and surface structure investigation for the positive electrodes of degraded lithium-ion cell after storage test using X-ray absorption near-edge structure measurement. *J. Power Sour.* **189**, 676-680 (2009).
166. P. Mukherjee *et al.*, From Nanometer to Atomic Resolution X-ray EDS analysis of Al in Ni-rich Layered Oxide Li-Ion Cathodes. *Microsc. Microanal.* **23**, 386-387 (2017).
167. E. A. Zvereva *et al.*, Monoclinic honeycomb-layered compound $\text{Li}_3\text{Ni}_2\text{SbO}_6$: preparation, crystal structure and magnetic properties. *Dalton Trans.* **41**, 572-580 (2012).
168. E. McCalla *et al.*, Understanding the Roles of Anionic Redox and Oxygen Release during Electrochemical Cycling of Lithium-Rich Layered $\text{Li}_4\text{FeSbO}_6$. *J. Am. Chem. Soc.* **137**, 4804-4814 (2015).
169. M. Sathiya *et al.*, $\text{Li}_4\text{NiTeO}_6$ as a positive electrode for Li-ion batteries. *Chem. Commun.* **49**, 11376-11378 (2013).
170. R. a. D. Clos, M. and Hagenmuller, P. and Hoppe, R. Paletta, E., Sur quelques oxydes doubles de potassium et de lanthanides de formule KLnO_2 , a structure NaFeO_2 alpha. *C. R. Hebd. Seances Acad. Sci.* **265**, 801-804 (1967).
171. C. Vaalma, G. A. Giffin, D. Buchholz, S. Passerini, Non-Aqueous K-Ion Battery Based on Layered $\text{K}_{0.3}\text{MnO}_2$ and Hard Carbon/Carbon Black. *J. Electrochem. Soc.* **163**, A1295-A1299 (2016).

172. H. Kim *et al.*, Investigation of Potassium Storage in Layered P3-Type $K_{0.5}MnO_2$ Cathode. *Adv. Mater.* **29**, 1702480 (2017).
173. C. Delmas, C. Fouassier, Les Phases K_xMnO_2 ($x \leq 1$). *Zeitschrift für anorganische und allgemeine Chemie* **420**, 184-192 (1976).
174. Y. Hironaka, K. Kubota, S. Komaba, P2- and P3- K_xCoO_2 as an electrochemical potassium intercalation host. *Chem. Commun.* **53**, 3693-3696 (2017).
175. M. Pollet *et al.*, Structure and Properties of Alkali Cobalt Double Oxides $A_{0.6}CoO_2$ ($A = Li, Na, \text{ and } K$). *Inorg. Chem.* **48**, 9671-9683 (2009).
176. C. Liu *et al.*, $K_{0.67}Ni_{0.17}Co_{0.17}Mn_{0.66}O_2$: A cathode material for potassium-ion battery. *Electrochem. Commun.* **82**, 150-154 (2017).
177. T. Masese *et al.*, Rechargeable potassium-ion batteries with honeycomb-layered tellurates as high voltage cathodes and fast potassium-ion conductors. *Nat. Commun.* **9**, 3823 (2018).

Acknowledgments: Funding: This work was supported by the National Natural Science Foundation of China (51725206, 51421002, 21773303), the Strategic Priority Research Program of the Chinese Academy of Sciences (XDA21070500), Beijing Municipal Science and Technology Commission (Z181100004718008), and the Netherlands Organization for Scientific Research (NWO) under the VICI grant nr. 16122. Computations were performed on the niagara supercomputer at the SciNet HPC Consortium. SciNet is funded by: the Canada Foundation for Innovation; the Government of Ontario, Ontario Research Fund-Research Excellence, and the University of Toronto. C. Zhao also thanks to the State Scholarship Fund of China Scholarship Council (CSC). **Author contributions:** Y.-S.H. conceived this research and supervise this work with M.W., C.Z. and Q.W. whom conceptualized the ionic potential method and developed the calculation on examples of Na-/Li-/K-ion layered oxides. C.Z. and Q.W. performed synthesis procedures, experimental investigation of $NaLi_{1/3}Ti_{1/6}Mn_{1/2}O_2$ and $Na_{5/6}Li_{5/18}Mn_{13/18}O_2$ materials, software programming to process and present collected data. F.D. synthesize the Na-Li-Cu-Fe-Mn-O materials. Z.Y. B.S.L., and A.A.G. predict Na-ion layered oxides tested by cationic potential. J.W. and X.B. performed STEM observation and analysis. C.Z., Q.W., Z.Y., M.W., Y.L., C.D., and Y.-S.H. wrote the manuscript. All authors participated in analysing the experimental results and preparing the manuscript. C.Z., Q.W., and Z.Y. contributed equally to this work. **Competing interests:** All authors declare that they have no competing interests. **Data and materials availability:** All data is available in the main text or the supplementary materials.

Supplementary Materials:

Materials and Methods

Supplementary Text

Figures S1-S15

Tables S1-S19

References (24-177)